Author Manuscript

Author Manuscript

Author Manuscript

Author Manuscript

HHS Public Access

Author manuscript

Ann Biomed Eng. Author manuscript; available in PMC 2018 February 01.

Published in final edited form as:

Ann Biomed Eng. 2017 February ; 45(2): 360–377. doi:10.1007/s10439-016-1619-1.

Optimizing Photo-encapsulation Viability of Heart Valve Cell Types in 3D Printable Composite Hydrogels

Laura Hockaday Kang, **Patrick Armstrong**, **Lauren Lee**, **Bin Duan**, **Kevin Heeyong Kang**, and **Jonathan Talbot Butcher**

Abstract

Photocrosslinking hydrogel technologies are attractive for the biofabrication of cardiovascular soft tissues, but 3D printing success is dependent on multiple variables. In this study we systematically test variables associated with photocrosslinking hydrogels (photoinitiator type, photoinitiator concentration, and light intensity) for their effects on encapsulated cells in an extrusion 3D printable mixture of methacrylated gelatin/poly-ethylene glycol diacrylate/alginate (MEGEL/PEGDA3350/alginate). The fabrication conditions that produced desired hydrogel mechanical properties were compared against those that optimize aortic valve or mesenchymal stem cell viability. In the 3D hydrogel culture environment and fabrication setting studied, Irgacure can increase hydrogel stiffness with a lower proportional decrease in encapsulated cell viability compared to VA086. Human adipose derived mesenchymal stem cells (HADMSC) survived increasing photoinitiator concentrations in photo-encapsulation conditions better than aortic valve interstitial cells (HAVIC) and aortic valve sinus smooth muscle cells (HASSMC). Within the range of photo-encapsulation fabrication conditions tested with MEGEL/PEGDA/alginate (0.25–1.0% w/v VA086, 0.025–0.1% w/v Irgacure 2959, and 365 nm light intensity 2–136 mW/cm^2), the highest viabilities achieved were 95%, 93%, and 93% live for HASSMC, HAVIC, and HADMSC respectively. These results identify parameter combinations that optimize cell viability during 3D printing for multiple cell types. These results also indicate that general oxidative stress is higher in photocrosslinking conditions that induce lower cell viability. However, suppressing this increase in intracellular oxidative stress did not improve cell viability, which suggests that other stress mechanisms also contribute.

Key Terms

Hydrogel; extrusion bioprinting; oxidative stress; aortic valve interstitial cells; aortic valve smooth muscle cells; PEGDA; gelatin; mesenchymal stem cells; photo-polymerization; bio-ink; biofabrication

Corresponding Author: Jonathan T Butcher, PhD, Associate Professor and Associate Director, Nancy E. and Peter C. Meinig School of Biomedical Engineering, 304 Weill Hall, Cornell University Ithaca NY 14850, Phone: 607 255-3575, Fax: (607) 255-7330, jtb47@cornell.edu.

Disclosure Statement

No competing financial interests exist.

Author Manuscript Author Manuscript Author Manuscript Author Manuscript

3. Introduction

Heart valve disease is a tremendous and rising global burden[26]. For a pediatric patient, the prosthetic replacement of a congenitally-malformed or disease-destroyed heart valve is accompanied by risks associated with anticoagulant treatment and resizing surgeries[29]. As a result, researchers are working to use tissue engineering to address the need for a non-thrombogenic and non-immunogenic valve replacement that would integrate and grow with the patient. Towards this goal, hydrogel materials are being combined with nontraditional molding, electrospinning, or additive manufacturing fabrication strategies[14,18,24,46] to better control geometry, structure, and cell behavior within engineered valves. Many of the hydrogel technologies being developed and adapted to mimic the extracellular matrix (ECM) environment that cells inhabit in valve tissue utilize photocrosslinking[3,4,8,17,18,47,48,51]. By using photocrosslinking and 3D printing, a high degree of geometric control and shape fidelity of an implant scale hydrogel construct can be achieved[25]. Direct 3D bioprinting of cells into hydrogel valve constructs enables controlled deposition of cells within the structure[14]. However, encapsulation bioprinting in context of photocrosslinking requires that cells tolerate not only the solidified hydrogel, but also the printing solution and fabrication conditions including the polymer precursors, photoinitiator, products of initiation and propagation, and light exposure.

Poly-ethylene glycol (PEG)-based polymer precursors, methacrylated gelatin, and alginate have previously been used for the encapsulation of living cells[3,14,17]. PEG-based hydrogels have been used to study heart valve interstitial cell response to mechanical properties in both 2D and encapsulated 3D in-vitro studies[17,31]. The potential for mechanical and/or molecular customization and relatively low cost, makes PEG-based polymer precursors an attractive material component for scalable 3D tissue printing. Gelatin, a protein-rich matrix derived from collagen, provides cell attachment binding domains and can be modified to make photocrosslinking methacrylated gelatin (MEGEL)[3]. MEGEL hydrogels are enzymatically degradable and can encapsulate valve interstitial cells[3]. The addition of poly-(ethylene glycol)diacrylate (PEGDA) allows for tunable mechanical properties[27]. Alginate has been used in extrusion 3D printing both as a viscosity modifier and as a hydrogel precursor[14,25]. In this study, PEGDA and MEGEL photocrosslinkable hydrogel precursors were combined with non-photo-crosslinking alginate to make a solution suitable for extrusion 3D bioprinting.

Researchers have observed cell-specific differences in response to photoinitiator radicals[50] and different amounts/expression of intracellular and membrane components can engender protection against oxidative stress[34]. Valve interstitial cells (VIC) and sinus smooth muscle cells (SSMC) are the main cell types that populate valve leaflets and root wall of the valve [7] and have been used to study mechanistic and remodeling behavior as well as to establish tissue engineering targets [15,21,45]. Adipose derived mesenchymal stem cells (ADMSC) are a potentially feasible cell source for adult and pediatric tissue engineered heart valves (TEHV)[10]. We hypothesized that the viability of human aortic valve interstitial cells (HAVIC), human aortic valve sinus smooth muscle cells (HASSMC) and human adipose derived mesenchymal stem cells (HADMSC) would be different following photo-encapsulation into MEGEL/PEGDA hydrogels. We further hypothesized that these cell types

Author Manuscript Author Manuscript Author Manuscript Author Manuscript

are endowed with different or different amounts of protective intracellular membrane contents and therefore exposure to photoinitiator radicals would lead to differential intracellular oxidative stress between these different cells. For the purposes of tissue engineering, cells seeded into scaffolds and printed constructs must be viable in order to survive and function within the construct long term or eventually remodel and replace the scaffold. However, in the context of biofabrication strategies it is also important to also assess short term and immediate impact of fabrication parameters on cells to identify which parts of the strategy can be optimized[12,28]. In the present study, we used intact cell membranes and intracellular esterase activity (Live/Dead assay for mammalian cells) as a marker of viability to screen photo-encapsulation fabrication parameters for compatibility with valve cell and stem cells, from day 1 to 7 in culture. We hypothesized that Irgacure and VA086 photoinitiators could be used in sufficient amounts to enable solidification of a 1.5 mm thickness hydrogel precursor solution upon 5 minutes of exposure to a photo-crosslinking light source and achieve greater than 80% encapsulated cell viability. We chose these targets because this thickness of precursor solution approximately corresponds between two and three extrusion printed layers of hydrogel (if using a 0.8 mm diameter printing tip)[28], and could enable printing of a 3 cm tall hydrogel construct in 100 minutes (a scale useful if fabricating a heart valve conduit)[25]. Additionally, our previous work with a methacrylated gelatin and methacrylated hyaluronic acid photocrosslinking hydrogel prepared with Irgacure photoinitiator, demonstrated greater than 80% live/dead HAVIC and HADMSC viability at 14 and 28 days in culture[13], and VA086 photoinitiator is reportedly less cytotoxic than Irgacure[9,38]. In the present study we quantified the percentage of live HAVIC, HASSMC, and HADMSC in photo-crosslinking encapsulation conditions in MEGEL/PEGDA hydrogels with Irgacure 2959 and VA086 photoinitiators. Additionally, cells were loaded with 5-(and-6)-chloromethyl-2′,7′-dichlorodihydrofluorescein diacetate acetyl ester CM-H_2DCFDA (DCF), a general oxidative stress indicator, prior to encapsulation, to investigate the role of intracellular oxidative stress in cell-specific vulnerability to photo-crosslinking conditions. We also tested catalase treatment for its ability to prevent intracellular oxidative stress and rescue photo-encapsulated cells from photoinitiator induced damage.

4. Materials and Methods

Preparation of Sterile Polymer Precursor Solution

MEGEL[16] and polyethylene glycol diacrylate molecular weight 3350 (PEGDA3350)[11] were synthesized as previously described (Sigma-Aldrich Corp., St. Louis, MO, USA). After synthesis the polymers were dialyzed against distilled water for 1 week (dialysis tubing MW cut off of 1000 Da). The polymer product was then frozen at −20°C and subsequently lyophilized. Polymers were sterilized for 1 hour using germicidal UV. Photoinitiators 2,2′-Azobis[2-methyl-N-(2-hydroxyethyl)propionamide] (VA086, Wako Chemicals) and 2-hydroxy-1(4-(hydroxyethox)pheny)-2-methyl-1-propanone (Irgacure 2959, BASF Corporation, Newport, DE) were dissolved in 70% ethanol and sterile filtered to make stock solutions (0.1g VA086/ml, 0.015g Irgacure/ml)[9,38]. Irgacure photoinitiator was investigated because it has been one of the most widely used in contact with cells[19] and it has been previously used in the photo-encapsulation of both valve and adipose derived stem cells[13,15].

Author Manuscript Author Manuscript Author Manuscript Author Manuscript

VA086 photoinitiator was investigated because it is reportedly less cytotoxic compared to Irgacure[9,38]. Precursor solutions were made 20% w/v polymer to solution, MEGEL:PEGDA 3350 1:1. Stock solution and valve cell culture media was added to sterilized polymers to give a final concentration of 0.25–1.0% w/v VA086 or 0.025–0.1% w/v Irgacure then dissolved at 37°C.

Light Source and 3D Printing Platform

Three 365 nm light sources used in combination with the-Fab@Home™ Model 1 3D printing platform[25] were characterized with a UVX Radiometer (Supplemental Fig. S1 and Table S1). The lower intensity light sources were tested because we had previously found them effective for photocrosslinking other hydrogel precursor solutions[13,15,25] and we built and tested the high LED array light source so less efficiently crosslinking photoinitiator and polymer precursor combinations could be tested. To test a range, a high and a low light intensity (2 and 136 mW/cm$^{2)}$, were selected for mechanical testing and cell encapsulation. These correspond to a lamp (Fig. 1A) and a high powered LED array (HLED, Fig. 1B, C).

Mechanical Testing and Swelling Ratio of Hydrogel Disks

Mechanical properties of crosslinked hydrogels were tested to determine working ranges for fabrication. The goal is to determine if MEGEL/PEGDA hydrogels can mimic aortic valve mechanical properties, and to determine if after the minimum crosslinking of the precursor solution occurs to achieve hydrogel solidification, to what degree the hydrogel modulus affected by the photoinitiator concentration and light source intensity. Precursor solution was crosslinked into disks and rinsed for mechanical and swelling tests. Precursor solution was pipetted into a syringe, 7.5% w/v Protanal LF 10/60 sodium alginate (alginate, FMC, Philadelphia PA) was added as a viscosity modifier. The solution was extruded into silicone rubber 8 mm diameter, 1.5 mm high disk molds and leveled with a coverslip. The filled molds were exposed to 2 or 136 mW/cm^2 (lamp or HLED) of 365 nm light and crosslinked for 3, 5, and 7 min minutes. The crosslinked hydrogel disks were then hydrated in 1X phosphate buffered saline (PBS, VWR International, Radnor PA), placed on a rocker at room temperature, and PBS was exchanged after 1 and 24 hours to rinse out the alginate viscosity modifier. Disks were then mechanically tested or evaluated for swelling. Uniaxial confined compression testing was performed on a mechanical testing platform (EnduraTec 3200; Bose Electroforce, Eden Prairie, MN). Samples were ramp loaded quasi-statically at 0.01 mm/sec to 30% strain. Modulus (E_{5to15}) was calculated from the 5 to 15% strain portion of the stress strain curve. Sample size was n=3–14 and hydrogel thickness ranged from 1.5 mm to 2.0 mm. Disks designated for swelling tests were weighed to determine the equilibrium swollen mass, lyophilized for 48 hours, and weighed to obtain the dry polymer mass for each sample. The hydrogel swelling ratio based on mass was calculated [2] with the relationship:

$$Swelling\ Ratio\ (SR) = \frac{Wet\ Weight\ of\ Swollen\ Hydrogel\ Disk}{Dry\ Weight\ of\ Hydrogel}$$

Sample size was n=5–8.

Author Manuscript Author Manuscript Author Manuscript Author Manuscript

To compare crosslinked hydrogel mechanical properties against native tissue, aortic valve sinus tissue was tested. Adult porcine aortic valve conduit tissue was obtained fresh at slaughter (Shirk Meats, Himrod, NY), and 8 mm diameter biopsy tissue punches (Integra Miltex, York, PA) were used to sample the aortic sinuses of porcine aortic valves. Tissue was kept at 4°C in sterile PBS with protease inhibitor prepared with 1 protease inhibitor cocktail tablet in 50 ml of PBS, and mechanically tested within 48 hours of harvest (Roche Diagnostics, Indianapolis, IN). Ten sinus punches were taken from 3 pig aortic valves with a range of 1.3 to 1.9 mm in thickness and ramp loaded in compression (0.01 mm/sec, to 30% strain) to calculate E_{5to15}.

Heart Valve and Mesenchymal 2D Cell Culture and Expansion

Direct cell printing encapsulation conditions were tested for HAVIC, HASSMC, and Human ADMSC (HADMSC). HAVIC and HASSMC were isolated from the aortic valve of a donor heart[16]. Tissue was procured with consent as approved by the Institutional Review Board of Weill-Cornell Medical College in New York City. Cells were isolated via collagenase digestion as previously described[6], except that the collagenase used to digest leaflet and root tissue was made with MCDB 131 medium (Sigma) and the HASSMC were isolated from tissue below the sinotubule junction. Cryopreserved HADMSC were purchased (Lonza, Walkersville). Human valve cells were expanded and maintained in MCDB131 medium supplemented with 0.25 μg/L recombinant human fibroblast growth factor basic (rhFGF-2; Invitrogen) and 5 μg/L recombinant human epidermal growth factor (rhEGF; Invitrogen). HADMSC were expanded and maintained Nutrient Mixture F-12:Dulbecco's Modified Eagle Medium: (Invitrogen). All media were supplemented with 10% fetal bovine serum (Gemini Bio-products, Sacramento CA) and 1% penicillin/streptomycin (Invitrogen). Media was exchanged every 2–3 days. Cells were used at passage 4–8 when flasks reached 80–95% confluent.

Encapsulation and Handling for Disk Experiments and In vitro Culture

Cells were encapsulated in precursor solutions and crosslinked with either 2 or 136 mW/cm^2 light. Precursor solution was prepared as described above, with cells added into the warmed precursor solution ($2.5*10^6$ cells/ml) prior to the addition of alginate. Filled molds were exposed to UV light for 5 minutes, and 20 ml of media was applied to submerge, hydrate, and loosen the cell-hydrogel disks before the molds were removed. After 1 hour incubation in MCDB131 medium at 37°C, cell-hydrogel disks were transferred to 6-well plates containing fresh medium. Plates were placed on a rocker in an incubator (37°C and 5% CO_2). Medium was exchanged after 24 hours and subsequently every 48 hours. Hydrogel-cell disks were cultured on a rocker because the agitation helps to wash the alginate viscosity modifier and unreacted photoinitiator out of the crosslinked hydrogel.

LIVE/DEAD Staining

Cell-hydrogels were stained with LIVE/DEAD® viability assay calcein-AM/ethidium homodimer (Invitrogen, 2μM/4μM in PBS, 30 min, 37°C), and imaged using an epiflourescence stereomicroscope (SteREO Discovery.V20; Zeiss, Germany) to determine the percentage of cells with intact plasma membranes at 1, 3, 4, and 7 days of culture (ImageJ)[25]. Sample size was n=3–4. Calcein-AM green fluorescent stain indicates

Author Manuscript Author Manuscript Author Manuscript Author Manuscript

intracellular esterase activity, and red-fluorescent ethidium homodimer-1 localizes to the cell nucleus when the plasma membrane is compromised. Cell circularity (index of cell spreading) was quantified using ImageJ to threshold images of the cells whose cytoplasm exhibits green fluorescence when stained with calcein-AM. The analyze particle circularity function was used and shapes larger than cell nuclei were selected for.

General Oxidative Stress

Encapsulated cells were labeled with 5-(and-6)-chloromethyl-2′,7′-dichlorodihydrofluorescein diacetate, acetyl ester CM-H_2DCFDA (DCF, Invitrogen) to indicate general oxidative stress and CellTracker™ Red CMTPX (CTR, Invitrogen) to tag all cells' cytoplasm. Prior to encapsulation $0.5*10^6$ cells/ml were incubated in DCF (10 μM), CTR (7 μM), and Hank's Balanced Salt Solution (HBSS, Invitrogen) working solution (20 min, 37°C)[30]. DCF-CTR-loaded cells were rinsed in HBSS, pelleted, and then mixed into polymer precursor solution (0.1% w/v Irgacure or 1.0% VA086, $2.5*10^6$ cells/ml) before alginate was mixed in. After 5 minutes of photocrosslinking, MCDB media was applied to cell-hydrogel disks. 1 ml of HBSS was pipetted into each well of a black bottom 48 well plate and the cell-hydrogel disks were transferred into the wells. Hydrogel-only and cell suspension controls of DCF-CTR-loaded cells suspended in HBSS were also transferred into wells. An area scan of each well (Ex/Em 485/528) for DCF fluorescence was performed using a multi-detection microplate reader (BioTek, Winooski VT). Disks were transferred back into media and incubated at 37°C and imaged using confocal laser scanning microscopy (25X H_2O objective, LSM 710, Carl Zeiss) (n=4 for all conditions). Image J image analysis was used to determine percent of cells experiencing oxidative stress (DCF+ cell count/CTR+ cell count *100).

Catalase Treatment of Cells

Catalase pre-treatment was tested as a strategy to mitigate photoinitiator induced cell damage and improve cell survival into the 80% live cell range for the more crosslinked hydrogel conditions. We hypothesized that catalase, an antioxidant that has previously been used to prevent hydrogen peroxide radical formation in smooth muscle cells[41], would neutralize or prevent oxidative damage inside photo-encapsulated cells and would have a positive effect on cell survival. To determine the effect of catalase on oxidative stress, cells were DCF/CTR loaded and encapsulated as described above with the addition of catalase (Sigma, 1000 units/ml of HBSS)[40,41] into the DCF/CTR/HBSS working solution. To determine the effect of catalase on viability, cells were incubated in catalase/HBBS solution, encapsulated the same way as the DCF-CTR loaded cells, and then assayed at day 3 of culture with LIVE/DEAD.

Oxidative stress ratios were calculated from fluorescence values of HBSS treated cell-laden hydrogels divided by catalase treated cell-laden hydrogels of a given photoinitiator and light source condition.

$$Oxidative\ Stress\ Ratio = \frac{Average\ HBSS\ Relative\ DCF\ Fluorescence}{Average\ Catalase\ Relative\ DCF\ Fluorescence}$$

Author Manuscript Author Manuscript Author Manuscript Author Manuscript

Hydrogel Precursor Solution as a Printable Ink

The MEGEL:PEGDA 3350 hydrogel precursor solution with alginate was specifically developed as an ink for bioprinting. To demonstrate this as an extrudable ink, the Fab@Home Model 1 printer was used to fabricate a hydrogel prism example geometry designed in vector format in Excel. HADMSC were labeled with either CTR (7 μM) or CellTracker Green CMFDA 5-chloromethylfluorescein diacetate (CTG, 7 μM, Invitrogen) before encapsulation into the hydrogel precursor solution. The precursor solution was printed into the test prism, photocrosslinked for 5 minutes at 2 mW/cm^2, and then cultured on a rocker. After 3 days of culture, the bioprinted prism was imaged with the epiflourescence stereomicroscope.

Statistics

Analysis of variance (ANOVA) was conducted on mechanical, viability, and oxidative stress data sets with Tukey honest significant difference (HSD) post hoc tests performed when there are more than two groups, and Student's t-test performed to compare between two groups (JMP PRO software). Means were considered significantly different $p<0.05$ and significance is indicated on graphs by non-matching letters. The results of the two-way and three-way ANOVA are included as supplemental tables. Standard error of the mean is displayed on graphs.

5. Results

Range of Mechanical Properties Induced by Photocrosslinking Conditions

MEGEL/PEGDA hydrogel precursor solution can be used as an extrusion bioprinting ink, which was demonstrated by printing red and green labeled HADMSC directly into a cell-laden square prism with internal lined heterogeneity (Fig. 1D). Strategies for photo-crosslinking include crosslinking during printing or crosslinking post fabrication of the whole construct. Whichever strategy is used, light exposure must be sufficient to solidify the hydrogel structure. To test assess the effects of variables associated with photocrosslinking cell ink precursor solutions were photocrosslinked into a simple disk geometry (Fig. 1E). If light exposure occurs during printing is being used in our syringe-carriage-mounted-LED array printing configuration, the distance varies between the light sources and construct as the syringes trace out the print paths, as the stage moves up and down when it initiates a new path, and as the stage moves down with each layer. Consequently, with a single output array, the energy delivery to the extruded precursor solution is not constant. The hydrogel formation, compressive modulus (E_{5to15}) and swelling ratio of photo-crosslinked MEGEL/PEGDA hydrogels were affected by light source intensity, photoinitiator type, and photoinitiator concentration (Fig. 2).

A range of hydrogel compressive moduli (E_{5to15} averaged 19.3±2.7 kPa to 120.7±10.2) result from the photocrosslinking conditions tested in the ranges of 0.25–1.0% w/v VA086 or 0.025–0.1% w/v Irgacure and 2–136 mW/cm^2 (Fig. 2). During hydrogel compression the stress response to strain is non-linear (Fig. 2A), and changing the photoinitiator and light source intensity produces hydrogels that follow 3 different profiles. E_{5to15} of hydrogels made with VA086 and photo-crosslinked for 5 min with the low intensity light source (2

Author Manuscript Author Manuscript Author Manuscript Author Manuscript

mW/cm^2) was not significantly affected by increasing the photoinitiator concentration except that at low photoinitiator concentration, a robust gel did not form (Fig. 2B, values in Table S2). A large fraction of hydrogel disk batches made with 0.25% w/v VA086 dissolved when transferred into PBS or media. Crosslinking for 0.5% w/v VA086 was inconsistent, but almost 100% for 0.75% w/v VA086. E_{5to15} of hydrogels made with Irgacure 2959, and photo-crosslinked for 5 min with the low intensity light source (2 mW/cm^2), was not significantly affected by increasing the photoinitiator concentration (Fig. 2C). For the lamp light intensity there appear to be saturation points, past which increased photoinitiator does not increase the modulus. Increasing the light intensity that precursor solution was exposed to for 5 min of crosslinking significantly increased the E_{5to15} for hydrogels made with both 1.0% w/v VA086 (26 kPa increase) and 0.1% w/v Irgacure (80 kPa increase) (Fig. 2D,2E). Comparable moduli between the two photoinitiators in the methacrylated gelatin hydrogels, were found at a ratio of 1 to 30. Concentrations 0.025% w/v Irgacure and 0.75% w/v VA086 with 5 minutes of 2 mw/cm^2 crosslinking resulted in hydrogel E_{5to15} (22.8±3.1 kPa and 20.0±3.9 kPa respectively) that were not significantly different from each other or from porcine aortic valve sinus tissue (E5to15=17.86±2.198 kPa) (One-Way ANOVA F ratio = 1.0532 p=0.3665, Tukey HSD post-hoc test no significant difference).

Hydrogel swelling ratio was affected by both the light intensity used for crosslinking and the photoinitiator concentration in hydrogels prepared with VA086 (Fig. 2F, Table S3). VA086 hydrogels were significantly less swollen with water when crosslinked at the higher intensity, and less swollen with water for the 1.0% w/v compared to 0.5%w/v condition. For the low photoinitiator Irgacure hydrogels (0.025% w/v) and the high photoinitiator hydrogels (0.1%w/v) increasing the intensity of light source did not significantly affect the swelling ratio (Fig. 2G). Increasing Irgacure photoinitiator concentration decreased how much the hydrogel would swell with water. Plotting the modulus against the swelling ratio (Fig. 2H) gives a trend that as swelling ratio decreases the modulus increases, supporting that the degree of photocrosslinking increases as the modulus increases.

Encapsulated Valve and Mesenchymal Cell Viability and Morphology

Encapsulated valve cells had significantly less viability and rounder morphology compared to mesenchymal stem cells in photo-crosslinked MEGEL:PEGDA hydrogels. The percentages of live HADMSC, HAVIC, and HASSMC were all affected by Irgacure photoinitiator concentration in the hydrogels photo-crosslinked at 2 mW/cm^2 and evaluated with Live/Dead at day 1 in culture (Fig. 3A, Table S2). At the VA086 concentrations tested, when precursor solution were photo-crosslinked at 2 mW/cm^2, HADMSC and HAVIC were not significantly affected by photoinitiator concentration but HASSMC were (Fig. 3B). At day 1 in culture there was a statistically significant interaction between the effect of cell type and the effect of photoinitiator concentration on the percentage of live cells in the Irgacure hydrogels (two-way ANOVA, F=5.894 p=0.0015) (Fig. 3A, Table S8). For hydrogels prepared with Irgacure at day 1 in culture the effect of photoinitiator concentration on the percentage of live cells depends on the cell type encapsulated, with photoinitiator concentration having a greater effect on HAVIC than on HADMSC and HASMC. At day 1 in culture there was a statistically significant interaction between the effects of cell type and VA086 photoinitiator concentration on the percentage of live cells (Fig. 3B, Table S9). The

Author Manuscript Author Manuscript Author Manuscript Author Manuscript

effect of VA086 photoinitiator concentration on the percentage of live cells depends on the cell type encapsulated (two-way ANOVA, F=3.96 p=0.0127), with photoinitiator concentration having a greater effect on HASSMC than on HADMSC and HAVIC.

Over the course of 7 days of culture, the viability of encapsulated HAVIC and HASSMC generally decreased the longer hydrogel disks made with 0.05 to 0.1%w/v Irgacure were cultured, while the percentage of live HADMSC was maintained (Fig. 3C, 3E, 3G, **two-way ANOVA results** Table S10, Table S12, Table S14). In general HAVIC and HADMSC viability is maintained in hydrogels prepared with 0.5 to 1%w/v VA086 (Fig. 3D, 3F, 3H, **two-way ANOVA results** Table S11, Table S13, Table S15). The percentage of live HASSMC decreased with day in culture in 1.0 %w/v VA086 condition but not the lower photoinitiator concentrations. As the result of this discovery that day in culture can affect the percentage of cells found alive in the hydrogels, day 3 instead of day 1 was used for the time point in the subsequent catalase and oxidative stress studies. These results suggest that compared to VA086, Irgacure by weight has a more detrimental effect on cell viability for both primary valve cells and adipose derived stem cells (Table S2).

At day 1 in culture the circularity of live cells depends on the cell type for hydrogels prepared with Irgacure and VA086 and photocrosslinked at 2 mw/cm^2 (Fig. 4, Table S2). At day 1 in culture there was a statistically significant interaction between the effect of cell type and the effect of Irgacure photoinitiator concentration on the circularity of live cells (F=7.5042 p=0.0003*, Table S16). Encapsulated HADMSC had a significantly more spread morphology compared to HAVIC and HASSMC in these Irgacure hydrogels, and HAVIC circularity increased with increasing photoinitiator concentration (Fig. 4A). At day 1 in culture there was not a statistically significant interaction between the effect of cell type and the effect of VA086 photoinitiator concentration on the circularity of live cells (F=1.8884 p=0.1438, Table S17). However, at day 1 in culture for hydrogels prepared with VA086, the circularity of live cells does depend on the cell type (p<0.0001) and encapsulated HAVIC are more round than HADMSC and HASSMC (Fig. 4B).

Catalase Treatment Reduces General Oxidative Stress

Hydrogels prepared at the highest photoinitiator concentrations tested in this study, Irgacure 0.1% w/v and VA086 1.0% w/v, had the most pronounced differences in encapsulated cell viability between cell-type (Fig. 3). DCF fluorescence indicates that general oxidative stress was induced in HADMSC, HAVIC, and HASSMC in these encapsulation conditions. In a given condition, not all cells were positive for oxidative stress, and the degree of oxidative stress in each cell varied. Fig. 5 and Table S4 summarizes the percentage of cells with positive DCF fluorescence and the relative DCF fluorescence intensity of gels laden with encapsulated cells.

For cells treated with HBSS control solution prior to encapsulation and then exposed to either lamp of high-power LED photo-crosslinking for 5 min, there was no significant difference in the percentage of cell experiencing oxidative stress between cell types in either Irgacure or VA086 photoinitiator condition (Fig. 5A and Fig. 5B, representative images in supplement Fig. S8). Directly after photo-crosslinking at the high light intensity (136 mW/cm^2), the DCF relative fluorescence of cell-hydrogel disks was significantly different

Author Manuscript Author Manuscript Author Manuscript Author Manuscript

between cell types for Irgacure and VA086 hydrogels prepared with HBSS control-treated cells (Fig. 5C, Fig. 5D, and Fig. 5E). HADMSC hydrogels were significantly less fluorescent than HAVIC and HASSMC in Irgacure hydrogels at both the high and low light intensities (Fig. 5C). In VA086 hydrogels, HADMSC and HAVIC hydrogels were less fluorescent than HASSMC hydrogels in 136 mW/cm^2 conditions (Fig. 5D), and HADMSC and HAVIC hydrogels were less fluorescent than HASSMC hydrogels in 2 mW/cm^2 conditions (Fig. 5E). The relative fluorescence measurements of the VA086/HLED conditions were not directly compared to the VA086/Lamp conditions due to differences in hydrogel foaming during crosslinking. The VA086 photoinitiator foams the hydrogel upon photocrosslinking with small gas bubbles throughout the hydrogel, and the HLED/VA086 condition is more buoyant compared to the lamp/VA086 conditions soon after photocrosslinking. As a result the HLED/VA086 condition fluorescence signal is more intense due to a buoyancy of the hydrogels in the well-plate and shorter distance to the well-plate reader detector (top-down detector setup, see schematic in Fig. S9).

Within each cell type, the percentage of cells experiencing oxidative stress induced by the high power LED array compared to the lamp was not significantly different (Fig. 5A and Fig. 5B). Catalase treatment prior to encapsulation dramatically decreased the percentage of HADMSC, HAVIC, and HASSMC experiencing intracellular general oxidative stress in both 2 and 136 mW/cm^2 intensity conditions. Within cell types there was not a significant difference in Irgacure hydrogel DCF fluorescence between the high power LED array compared to the lamp for HAVIC and HADMSC, but DCF fluorescence was less for HASSMC hydrogel conditions exposed to lamp compared to the high power LED (Fig. 5C). Catalase decreased the DCF relative fluorescence oxidative stress response in all 3 cell types, at 2 mW/cm^2 and 136 mW/cm^2, and with Irgacure and VA086 conditions (Fig 5A–E).

Effect of Catalase Treatment on Cell Viability and Morphology

In general catalase treatment did not improve 3 day encapsulated cell viability (Fig. 6, Table S4). In high and low light intensity crosslinking conditions catalase treatment was detrimental to HASSMC and was detrimental to HADMSC in Irgacure hydrogels, evidenced by a lower percentage of live cells (Fig. 6A). In high and low intensity crosslinking conditions catalase treatment did not significantly affect or improve HADMSC and HAVIC the percentage of live cells in VA086 hydrogels (Fig. 6B). Catalase treatment decreased the percentage of live HASSMC in low intensity crosslinking conditions in VA086 hydrogels. Circularity was unaffected by catalase treatment for HAVIC and HADMSC in Irgacure and VA086 hydrogels at both high and low light exposure conditions (Fig. 6C and Fig. 6D). HASSMC circularity was higher in catalase treatment groups (cells were more round) compared to HBSS controls in both Irgacure and VA086 hydrogels in only the low light intensity crosslinking conditions (Fig. 6C and Fig. 6D), and was not affected in the high light intensity crosslinking conditions. Increasing the light source intensity from 2 mW/cm^2 to 136 mW/cm^2 significantly decreased encapsulated cell viability in only one condition, HASSMC in VA086 hydrogels (Fig. 6B, Table S5).

Author Manuscript Author Manuscript Author Manuscript Author Manuscript

Oxidative Stress Ratio

The percentage of cells positive for general oxidative stress in a given photo-encapsulation condition was not significantly different between the three cell types. However, relative DCF fluorescence intensity measurements of cell-hydrogels indicate that encapsulated HAVIC and HASSMC are more fluorescent compared to HADMSC and therefore have more oxidation occurring within their cytoplasm in these same conditions. This suggests that the degree of general oxidative stress is greater or more acute in those cell types. Oxidative stress ratio (HBSS control divided by catalase treated in the same photo-encapsulation condition) was calculated as a strategy to normalize the relative DCF fluorescence intensity so the degree of oxidative stress experienced in a given condition could plotted be against the percentage of live cells in a given condition. The buoyancy and foaming of VA086 hydrogels made plotting relative DCF fluorescence directly against viability inappropriate. Oxidative stress ratio is higher for nearly all HAVIC and HASSMC conditions compared to HADMSC. Percentage of live cells at day 3 was plotted against oxidative stress ratio (Fig. 6E). The percentage of live cells decreases as oxidative stress ratio increases for individual cell types and independent of cell type. The studies with DCF indicate that general oxidative stress is higher in photocrosslinking conditions that induce lower cell viability. However, elimination of that oxidative stress does not increase cell viability, which suggests that intracellular oxidative stress is not the primary mode or most important symptom of damage caused by photocrosslinking conditions.

6. Discussion

Hydrogel materials are being explored as part of tissue engineering heart valve strategies[14,18,24,46–48,51]. Hydrogels have recently been used to form starter scaffolds that are rapidly remodeled by cells then decellularized to form implantable valves[46]; to mimic the native ECM environment and better hold cells within electrospun engineered valves[18,24]; and to incorporate regional matrix or mechanical differences directly into engineered valves[14,24]. Additionally, hydrogels are being used to control and study heart valve cell response to mechanical[17,31] and biochemical cues[3]. As novel material combinations are developed or materials are used in an unprecedented way, a major challenge is adapting hydrogel technologies into an effective fabrication strategies that maximize cell viability. The findings of our study identify parameter combinations that will help optimize cell viability during 3D bioprinting of cellularized hydrogels. MEGEL and PEGDA 3350 combined with alginate viscosity modifier and either Irgacure 2959 or VA086 photoinitiator, maintained at 37°C, is a 3D printable and photo-crosslinkable precursor mixture that can be used for encapsulated bioprinting/direct extrusion cell printing. We found that a range of photoinitiator concentrations and light source intensities could produce a crosslinked hydrogel from a 1.5 mm depth precursor solution with 5 minutes of light exposure that was robust enough for handling and culture for at least 1 week with encapsulated cells. Critically, light intensity measurements were taken and the hydrogel precursor solutions were exposed to light at the same distance from the source used in our printer when the extrusion tip is in contact with the printing surface and the light source is mounted on the syringe carriage. Hydrogel stiffness and swelling ratio were marginally tunable using photoinitiator type, photoinitiator concentration, UV light source intensity, and UV exposure time. HADMSC,

Author Manuscript Author Manuscript Author Manuscript Author Manuscript

HAVIC, and HASSMC survived the range of encapsulation conditions (photoinitiator concentrations, light source intensities, and hydrogel mechanical properties) tested in this study to different degrees. When cytotoxicity per gram of photoinitiator in solution is the only consideration, our results agree with previous studies[9,38] that Irgacure is more cytotoxic than VA086. If the only goal is enough crosslinking to reliably solidify extruded hydrogel, cell-hydrogel disks prepared with VA086 (0.75%w/v) or Irgacure (0.05%w/v) can achieve greater than the target 80% viability at day 1 for all three cell types. However, if more than minimum crosslinking in the hydrogel is desirable, then higher cytotoxicity is weighed against the effectiveness of the photoinitiator at crosslinking hydrogel precursors. Our results also indicate that Irgacure in a 3D hydrogel environment can give more mechanical gain with less detriment to encapsulated cells compared to VA086. Additionally, the percentage of live encapsulated HADMSC was always greater than or equal to the valve cell types in the photo-encapsulation hydrogel conditions tested here. Our results suggest that valve cells are more likely to die as the result of photoinitiator radical attack while stem cells are inherently less vulnerable. General oxidative stress was higher in the cell types that experienced lower encapsulated cell viability, and oxidative stress was higher in the photocrosslinking conditions that induced lower cell viability. However, suppressing this increase in oxidative stress did not increase cell viability, which suggests that intracellular oxidative stress is not the primary mode or most important symptom of damage caused by photocrosslinking conditions.

For the low light intensity, our data indicates there is a point past which increasing the photoinitiator did not significantly increase MEGEL/PEGDA hydrogel stiffness in the 5 to 15% strain range. Increasing the light intensity exposure of initiator-saturated precursor solution increased the stiffness of the hydrogels for both VA086 and Irgacure hydrogels. A cell-damage to mechanical-gain ratio can be calculated for a photoinitiator/polymer combination and cell type (Table1). This ratio is useful to emphasize cell-type dependent sensitivity to photoinitiators while also elucidating that VA086 can produce a less crosslinked hydrogel with equivalent or greater detrimental effects on cell viability when compared to Irgacure under specific 3D conditions. Identifying how to achieve sufficient rate and necessary degree of crosslinking of a hydrogel while balancing the viability of encapsulated cells is important for the successful application of biofabrication technologies that use photoinitiators. Mironi-Harpaz et al. recently used photolithographic 3D printing to pattern mechanically heterogeneous hydrogels in the presence of encapsulated cells[35], building from a previous study where they specifically evaluated effective crosslinking and cytotoxicity in conjunction with effective photopolymerization[36]. The cytotoxicity study evaluated three different photoinitiators (including Irgacure 2959) and bovine aortic smooth muscle cells in a PEGDA/PEG-fibrinogen hydrogel, and demonstrated that optimizing the concentration of photoinitiator to produce rapid and efficient crosslinking during a short photo-exposure time was important to minimize total time cells were exposed to photoinitiator radicals[36]. Our present data corroborates the conclusion that minimizing contact with photoinitiator radicals helps minimize detrimental effect on hydrogel encapsulated cell viability. Our further investigations, evaluation of more than one cell type for a longer culture time, reveal that different cell types when exposed to the same increase in photoinitiator radicals do not exhibit the same encapsulated viability.

Author Manuscript Author Manuscript Author Manuscript Author Manuscript

Tuning hydrogels to match the mechanical properties of native valves or stimulate specific valve cell functions is a critical idea in the field of tissue engineering[15,17,31]. The hydrogels and valve tissue are non-linear, and the compressive modulus of sinus tissue isolated from porcine aortic valves and the lowest modulus Irgacure and VA086 MEGEL/PEGDA3350 hydrogels disks were comparable. While the MEGEL/PEGDA3350 hydrogel precursor ink may be appropriate for aortic sinus region of heart valves, more compliant regions of engineered valves may need to be fabricated with a different ink formulation. Although we found that modulus and swelling were marginally tunable to a higher compressive modulus by changing photoinitiator and light source, adjusting these variables to tune the mechanical properties of the hydrogels into a lower modulus range is not practical for this precursor mixture. For example precursor solutions prepared with lower amounts of VA086 (0.25 and 0.5 w/v%) that were exposed to 2 mw/cm2 UV light for 5 minutes did not reliably form hydrogel disks. Adjusting the molecular weight of the precursor polymers[25] or the precursor components[15] is likely a better strategy.

We investigated a range of Irgacure and VA086 concentrations that can produce similar mechanical property MEGEL/PEGDA hydrogels, using modulus and swelling ratio to indicate degree of crosslinking. Irgacure more efficiently photocrosslinks polymer precursors and is effective at weight fractions lower than VA086[9,38]. The modulus of printable MEGEL/PEGDA hydrogel becomes comparable at a higher VA086 concentration (1:30 Irgacure:VA086, 2 mW/cm^2, 5 min) than was observed in methacrylated alginate (1:10 Irgacure:VA086)[38] and in tripeptide L-arginine-glycine-L-aspartic acid (RGD) modified methacrylated alginate hydrogels (1:7.5)[9]. Between Irgacure and VA086 MEGEL/PEGDA hydrogel with comparable modulus, the day 3 and 4 encapsulated viability of HADMSC (90% versus 93%) HAVIC: (66% versus 92%), and HASSMC: (61% versus 81%) corresponds to viability observed for methacrylated alginate encapsulated chondrocytes at 2 days of culture by Roulliard et al. (70% versus 90%)[38]. In 2D, Irgacure is dramatically more detrimental than VA086 for chondrocytes (10% verses 85%)[38] and pre-adipocytes. (2% versus 82%)[9] at the weight ratios used to get comparable mechanical properties in 3D. 1 to 30 Irgacure 2959 to VA086 gave comparable viability between the two photoinitiator types in a 2D study using human umbilical vein endothelial cells and bone marrow stromal cells[37]. Cytotoxicity in 3D encapsulation conditions may be less than in 2D culture because in the encapsulation conditions the cells, polymer precursors, and additives are all competing targets for the photoinitiator radicals[5,9,37,50].

Our results indicate that increasing the concentration of active photoinitiator radicals in the encapsulation conditions decreased cell viability. We found that HAVIC and HASSMC experience more general oxidative stress than HADMSC when encapsulated in photo-crosslinked hydrogels. Viability decreased as the intensity of oxidative stress experienced increases in photocrosslinking conditions. Other researchers have also observed cell specific sensitivity to photoinitiator toxicity and different toxicity of various photoinitiators[1,5,37,38,50], and have attributed encapsulated cell death to free radical damage[5]. Additionally, other researchers have shown free radical scavengers such as hydroquinone [1] and lactic acid[32], and protective antioxidant encapsulating nanoparticles [43] can mitigate radical cytotoxicity. However, interference with the hydrogel crosslinking, such as in the case of graphene oxide particles[42] or ascorbic acid[39], makes some radical-

Author Manuscript Author Manuscript Author Manuscript Author Manuscript

scavenging treatments strategies unsuitable for 3D printing. In the present study we investigated catalase pretreatment of cells prior to encapsulation as a strategy to reduce oxidative stress experienced by the cells without interfering with the crosslinking of the polymer precursor solution.

Treatment of HAVIC, HASSMC, and HADMSC with catalase prior to encapsulation almost eliminated general intracellular oxidative stress, and hydrogels were still able to crosslink. However, this treatment did not improve encapsulated HADMSC and HASSMC viability, but did slightly benefit HAVIC encapsulated viability. HASSMC, which experienced the highest oxidative stress, had the poorest viability response to oxidative stress suppression by catalase during photo-encapsulation. In conditions where more Irgacure photoinitiator radicals were produced, evidenced by an 80 kPa increase in the hydrogel modulus, intracellular oxidative stress did not significantly increase. These results indicate intracellular oxidative stress is not the primary mechanism of damage by VA086 and Irgacure radicals. While the catalase successfully reduced the intracellular oxidative stress in terms of hydrogen peroxide radicals, other types of oxidative stress that were not examined in this study could be causing critical damage. The plasma membrane in particular is still vulnerable to attack. Radicals produced by Irgacure are membrane impermeable and are suspected to cause damage by lipid peroxidation[5,20,32,50]. Less is known about the progression of VA086 radicals, but as an azo initiator it may also cause lipid peroxidation. The detection and rescue strategy demonstrated in the present study essentially addresses oxidation that propagates into or is present in the interior of the cell. Any lipid peroxidation occurring at the outer membrane of the cells, is unaddressed by this strategy and could be the most detrimental mode of damage. It has been demonstrated that a protective shell of pericellular matrix can improve chondrocyte viability in 3D photocrosslinking conditions[20], but for other cell types such as valve and stem cells, strategies to combat membrane lipid peroxidation could include treatment with membrane associating antioxidants[44], transfection to overexpress membrane antioxidants[34], and stimulation/recruitment of antioxidant enzymes to the plasma membrane[22]. If damage at the plasma membrane of the cell is the critical mode of damage, differences in plasma membrane components and proteins might explain cell-type-specific responses to photo-encapsulation conditions. Interestingly, ADMSC and VIC are non-uniform populations of cells expressing different proteins in their plasma membranes[33,49] so even within a cell type there would be differences in protection against photoinitiator radicals. It should also be noted that photoinitiator radical damage to the cell is likely not the only contributing factor to cell survival in these encapsulation conditions. It is important to appreciate that valve cells[17,31] and stem cells[15] are responsive to the stiffness of their environment. Although we are unable to decouple the effects of hydrogel modulus and photoinitiator radical damage on cells, over the course of 7 days in culture, the initial stiffness of the hydrogel negatively correlated with the percentage of live cells in the hydrogel to different degrees for each cell type. For HAVIC a negative correlation was present on day 1, 3, and 7. For HASSMC it was present on day 3 and 7, and for HADMSC it was present at day 3 (Fig. S11).

Within the range of photo-encapsulation fabrication conditions tested in this study using MEGEL/PEGDA/alginate precursor solution, high viabilities of three cells types relevant for TEHV could be obtained (89%, 91%, and 94% live for HASSMC, HAVIC, and HADMSC

Author Manuscript Author Manuscript Author Manuscript Author Manuscript

respectively) at day 1 of culture. These viabilities corresponded to the lowest degree of crosslinking that reliably formed a hydrogel with VA086 in the precursor solution. Based on our current understanding, if 3D printing a compliant construct, the minimum concentration of VA086 is recommended. However, if a higher power light source and a hydrogel with a E_{5to15} equal to and greater than 40 kPa is needed, Irgacure should be used. The photo-initiator and light source combinations that produce higher stiffness hydrogels, unfortunately reduce the percentage of live cells below the short term screening target of 80% live cells. Mitigating intracellular oxidative stress with catalase was not a successful strategy to improve cell viability in higher photoinitiator radical conditions. In fact, catalase treatment generally made cells more likely to die in the photo-encapsulation conditions tested. Future efforts should focus on identification of the cell-specific mechanism behind differential viability as the result of photo-encapsulation and the primary mode of damage. Identifying the primary mode of damage by VA086 and Irgacure photoinitiator radicals and then mitigating those effects for different cell types in hydrogel would greatly expand the application of 3D printing technology. The present study indicates that poorly chosen photocrosslinking conditions used to solidify precursor inks into hydrogels, can compromise cell membranes and induce cell death in encapsulated cells within the initial 1 to 7 days of culture. However, the timeline of cell damage and subsequent cell response needs to be further investigated. Other investigators characterizing biofabrication strategies, have found different factors contribute to cell survival, and these factors act or become effective at different timescales. For example Cui et al. found that their inkjet printing method produced transient membrane disruption in Chinese hamster ovary cells and cells could repair their membranes within two hours[12]. While investigating stereolithographic fabrication of cell populated hydrogels, Chan et al. found that sub-optimal available adhesion sites within PEGDA and RGD peptide hydrogels had a significant effect on encapsulated viability after day 4 in culture, but the molecular weight of hydrogel precursors could affect encapsulated cell viability by the first day in culture. The critical mode of damage from the photoinitiator radicals in our system might be very rapid, but the downstream response of the cells to that damage and their response to the material they are encapsulated in could take longer to evidence. Moving forward towards a bioprinted TEHV, additional functional markers beyond membrane integrity should be evaluated including valve cell phenotypic markers, cell proliferation, and extracellular matrix production at longer time points. Additionally, there are other photoinitiators being explored for cell encapsulation in PEG-based hydrogels, for example lithium phenyl-2,4,6-trimethylbenzoylphosphinate (LAP)[19] and eosin-Y [23]. Although a path forward may involve the adoption of more effective and cell compatible photoinitiators than either Irgacure 2959 or VA086, it is important build off the present study and continue to evaluate fabrication parameters in the context of cell viability.

Supplementary Material

Refer to Web version on PubMed Central for supplementary material.

Acknowledgments

This research was performed at Cornell University, in the Nancy E. and Peter C. Meinig School of Biomedical Engineering; 101 Weill Hall Cornell University Ithaca, NY 14853

Author Manuscript Author Manuscript Author Manuscript Author Manuscript

We thank Jhalak Agarwal and Jennifer Richards who helped develop hydrogel and cell handling protocols. We thank Shivaun Archer, Claudia Fischbach, Jennifer Puetzer, Jeffery Ballyns, Lawrence Bonassar, Paula Miller, Michael Shuler, and Sam Portnoff (Widetronix Inc.) for their assistance and sharing of equipment. We thank Luke and Naomi Shirk for providing porcine tissue for the early cell isolation and encapsulation studies. This research was supported by the Morgan Family, Felton Family Endowment for Human Heart Valve Research at Seattle Children's Hospital, Hartwell Foundation, National Science Foundation (CBET-0955172), NSF Graduate Research Fellowship, and American Heart Association (AH0830384N and 13POST17220071).

Abbreviations

CTR	CellTracker™ Red CMTPX
DCF	5-(and-6)-chloromethyl-2′,7′-dichlorodihydrofluorescein diacetate, acetyl ester CM-H_2DCFDA
E_{5to15}	compressive modulus calculated from the 5 to 15% strain
ECM	extracellular matrix
HADMSC	human adipose derived mesenchymal stem cells
HASSMC	human aortic valve sinus smooth muscle cells
HAVIC	human aortic valve interstitial cells
HBSS	Hank's Balanced Salt Solution
HLED	high powered light emitting diode
Irgacure 2959	2-hydroxy-1(4-(hydroxyethox)pheny)-2-methyl-1-propanone
LED	light emitting diode
MEGEL	methacrylated gelatin
PBS	phosphate buffered saline
PEG	poly-ethylene glycol
PEGDA	poly-ethylene glycol diacrylate
3D	three dimensional
TEHV	tissue engineered heart valves
2D	two dimensional
UV	ultraviolet
VA086	2,2′-Azobis[2-methyl-N-(2-hydroxyethyl)propionamide]

References

1. Atsumi T, Murata J, Kamiyanagi I, Fujisawa S, Ueha T. Cytotoxicity of photosensitizers camphorquinone and 9-fluorenone with visible light irradiation on a human submandibular-duct cell line in vitro. Arch Oral Biol. 1998; 43:73–81. [PubMed: 9569993]

Author Manuscript Author Manuscript Author Manuscript Author Manuscript

2. Baier Leach J, Bivens KA, Patrick CW Jr, Schmidt CE. Photocrosslinked hyaluronic acid hydrogels: Natural, biodegradable tissue engineering scaffolds. Biotechnology and Bioengineering. 2003; 82:578–589. [PubMed: 12652481]

3. Benton JA, DeForest CA, Vivekanandan V, Anseth KS. Photocrosslinking of gelatin macromers to synthesize porous hydrogels that promote valvular interstitial cell function. Tissue Eng Part A. 2009; 15:3221–3230. [PubMed: 19374488]

4. Benton JA, Fairbanks BD, Anseth KS. Characterization of valvular interstitial cell function in three dimensional matrix metalloproteinase degradable PEG hydrogels. Biomaterials. 2009; 30:6593–6603. [PubMed: 19747725]

5. Bryant SJ, Nuttelman CR, Anseth KS. Cytocompatibility of UV and visible light photoinitiating systems on cultured NIH/3T3 fibroblasts in vitro. J Biomater Sci Polym Ed. 2000; 11:439–457. [PubMed: 10896041]

6. Butcher JT, Nerem RM. Porcine aortic valve interstitial cells in three-dimensional culture: comparison of phenotype with aortic smooth muscle cells. J Heart Valve Dis. 2004; 13:478–485. discussion 485–476. [PubMed: 15222296]

7. Butcher JT, Simmons CA, Warnock JN. Mechanobiology of the aortic heart valve. J Heart Valve Dis. 2008; 17:62–73. [PubMed: 18365571]

8. Camci-Unal G, Aubin H, Ahari AF, Bae H, Nichol JW, Khademhosseini A. Surface-modified hyaluronic acid hydrogels to capture endothelial progenitor cells. Soft Matter. 2010; 6:5120–5126. [PubMed: 22368689]

9. Chandler EM, Berglund CM, Lee JS, Polacheck WJ, Gleghorn JP, Kirby BJ, Fischbach C. Stiffness of photocrosslinked RGD-alginate gels regulates adipose progenitor cell behavior. Biotechnol Bioeng. 2011; 108:1683–1692. [PubMed: 21328324]

10. Colazzo F, Sarathchandra P, Smolenski RT, Chester AH, Tseng YT, Czernuszka JT, Yacoub MH, Taylor PM. Extracellular matrix production by adipose-derived stem cells: implications for heart valve tissue engineering. Biomaterials. 2011; 32:119–127. [PubMed: 21074262]

11. Cruise GM, Scharp DS, Hubbell JA. Characterization of permeability and network structure of interfacially photopolymerized poly(ethylene glycol) diacrylate hydrogels. Biomaterials. 1998; 19:1287–1294. [PubMed: 9720892]

12. Cui X, Dean D, Ruggeri ZM, Boland T. Cell damage evaluation of thermal inkjet printed Chinese hamster ovary cells. Biotechnol Bioeng. 2010; 106:963–969. [PubMed: 20589673]

13. Duan B, Hockaday LA, Das S, Xu C, Butcher JT. Comparison of Mesenchymal Stem Cell Source Differentiation Toward Human Pediatric Aortic Valve Interstitial Cells within 3D Engineered Matrices. Tissue Eng Part C Methods. 2015; 21:795–807. [PubMed: 25594437]

14. Duan B, Hockaday LA, Kang KH, Butcher JT. 3D bioprinting of heterogeneous aortic valve conduits with alginate/gelatin hydrogels. J Biomed Mater Res A. 2013; 101:1255–1264. [PubMed: 23015540]

15. Duan, B., Hockaday, LA., Kapetanovic, E., Kang, KH., Butcher, JT. Stiffness and adhesivity control aortic valve interstitial cell behavior within hyaluronic acid based hydrogels. Acta Biomaterialia. 2013. http://dx.doi.org/10.1016/j.actbio.2013.1004.1050

16. Duan B, Kapetanovic E, Hockaday LA, Butcher JT. Three-dimensional printed trileaflet valve conduits using biological hydrogels and human valve interstitial cells. Acta Biomater. 2014; 10:1836–1846. [PubMed: 24334142]

17. Durst CA, Cuchiara MP, Mansfield EG, West JL, Grande-Allen KJ. Flexural characterization of cell encapsulated PEGDA hydrogels with applications for tissue engineered heart valves. Acta Biomater. 2011; 7:2467–2476. [PubMed: 21329770]

18. Eslami M, Vrana NE, Zorlutuna P, Sant S, Jung S, Masoumi N, Khavari-Nejad RA, Javadi G, Khademhosseini A. Fiber-reinforced hydrogel scaffolds for heart valve tissue engineering. J Biomater Appl. 2014; 29:399–410. [PubMed: 24733776]

19. Fairbanks BD, Schwartz MP, Bowman CN, Anseth KS. Photoinitiated polymerization of PEG-diacrylate with lithium phenyl-2,4,6-trimethylbenzoylphosphinate: polymerization rate and cytocompatibility. Biomaterials. 2009; 30:6702–6707. [PubMed: 19783300]

Author Manuscript Author Manuscript Author Manuscript Author Manuscript

20. Farnsworth N, Bensard C, Bryant SJ. The role of the PCM in reducing oxidative stress induced by radical initiated photoencapsulation of chondrocytes in poly(ethylene glycol) hydrogels. Osteoarthritis Cartilage. 2012; 20:1326–1335. [PubMed: 22796510]
21. Gould ST, Anseth KS. Role of cell-matrix interactions on VIC phenotype and tissue deposition in 3D PEG hydrogels. J Tissue Eng Regen Med. 2013
22. Hagmann H, Kuczkowski A, Ruehl M, Lamkemeyer T, Brodesser S, Horke S, Dryer S, Schermer B, Benzing T, Brinkkoetter PT. Breaking the chain at the membrane: paraoxonase 2 counteracts lipid peroxidation at the plasma membrane. FASEB J. 2014; 28:1769–1779. [PubMed: 24421402]
23. Hao Y, Shih H, Muňoz Z, Kemp A, Lin CC. Visible light cured thiol-vinyl hydrogels with tunable degradation for 3D cell culture. Acta Biomaterialia. 2014; 10
24. Hinderer S, Seifert J, Votteler M, Shen N, Rheinlaender J, Schäffer TE, Schenke-Layland K. Engineering of a bio-functionalized hybrid off-the-shelf heart valve. Biomaterials. 2014; 35:2130–2139. [PubMed: 24333025]
25. Hockaday LA, Kang KH, Colangelo NW, Cheung PY, Duan B, Malone E, Wu J, Girardi LN, Bonassar LJ, Lipson H, Chu CC, Butcher JT. Rapid 3D printing of anatomically accurate and mechanically heterogeneous aortic valve hydrogel scaffolds. Biofabrication. 2012; 4:035005. [PubMed: 22914604]
26. Howell EJ, Butcher JT. Valvular heart diseases in the developing world: Developmental biology takes center stage. The Journal of heart valve disease. 2012; 21:234–240. [PubMed: 22645860]
27. Hutson CB, Nichol JW, Aubin H, Bae H, Yamanlar S, Al-Haque S, Koshy ST, Khademhosseini A. Synthesis and characterization of tunable poly(ethylene glycol): gelatin methacrylate composite hydrogels. Tissue Eng Part A. 2011; 17:1713–1723. [PubMed: 21306293]
28. Kang KH, Hockaday LA, Butcher JT. Quantitative optimization of solid freeform deposition of aqueous hydrogels. Biofabrication. 2013; 5:035001. [PubMed: 23636927]
29. Karamlou T, Jang K, Williams WG, Caldarone CA, Van Arsdell G, Coles JG, McCrindle BW. Outcomes and associated risk factors for aortic valve replacement in 160 children: a competing-risks analysis. Circulation. 2005; 112:3462–3469. [PubMed: 16316968]
30. Kirkland RA, Saavedra GM, Franklin JL. Rapid activation of antioxidant defenses by nerve growth factor suppresses reactive oxygen species during neuronal apoptosis: evidence for a role in cytochrome c redistribution. J Neurosci. 2007; 27:11315–11326. [PubMed: 17942726]
31. Kloxin AM, Benton JA, Anseth KS. In situ elasticity modulation with dynamic substrates to direct cell phenotype. Biomaterials. 2010; 31:1–8. [PubMed: 19788947]
32. Lampe KJ, Namba RM, Silverman TR, Bjugstad KB, Mahoney MJ. Impact of lactic acid on cell proliferation and free radical-induced cell death in monolayer cultures of neural precursor cells. Biotechnol Bioeng. 2009; 103:1214–1223. [PubMed: 19408314]
33. Lin CS, Xin ZC, Deng CH, Ning H, Lin G, Lue TF. Defining adipose tissue-derived stem cells in tissue and in culture. Histol Histopathol. 2010; 25:807–815. [PubMed: 20376787]
34. Manevich Y, Sweitzer T, Pak JH, Feinstein SI, Muzykantov V, Fisher AB. 1-Cys peroxiredoxin overexpression protects cells against phospholipid peroxidation-mediated membrane damage. Proc Natl Acad Sci U S A. 2002; 99:11599–11604. [PubMed: 12193653]
35. Mironi-Harpaz I, Hazanov L, Engel G, Yelin D, Seliktar D. In-situ architectures designed in 3D cell-laden hydrogels using microscopic laser photolithography. Adv Mater. 2015; 27:1933–1938. [PubMed: 25655567]
36. Mironi-Harpaz I, Wang DY, Venkatraman S, Seliktar D. Photopolymerization of cell-encapsulating hydrogels: crosslinking efficiency versus cytotoxicity. Acta Biomater. 2012; 8:1838–1848. [PubMed: 22285429]
37. Occhetta P, Sadr N, Piraino F, Redaelli A, Moretti M, Rasponi M. Fabrication of 3D cell-laden hydrogel microstructures through photo-mold patterning. Biofabrication. 2013; 5:035002. [PubMed: 23685332]
38. Rouillard AD, Berglund CM, Lee JY, Polacheck WJ, Tsui Y, Bonassar LJ, Kirby BJ. Methods for photocrosslinking alginate hydrogel scaffolds with high cell viability. Tissue Eng Part C Methods. 2011; 17:173–179. [PubMed: 20704471]

Author Manuscript Author Manuscript Author Manuscript Author Manuscript

39. Sabnis A, Rahimi M, Chapman C, Nguyen KT. Cytocompatibility studies of an in situ photopolymerized thermoresponsive hydrogel nanoparticle system using human aortic smooth muscle cells. J Biomed Mater Res A. 2009; 91:52–59. [PubMed: 18690661]
40. Sakai S, Liu Y, Mah EJ, Taya M. Horseradish peroxidase/catalase-mediated cell-laden alginate-based hydrogel tube production in two-phase coaxial flow of aqueous solutions for filament-like tissues fabrication. Biofabrication. 2013; 5:015012. [PubMed: 23319520]
41. Sakata N, Miyamoto K, Meng J, Tachikawa Y, Imanaga Y, Takebayashi S, Furukawa T. Oxidative damage of vascular smooth muscle cells by the glycated protein-cupric ion system. Atherosclerosis. 1998; 136:263–274. [PubMed: 9543097]
42. Shin SR, Aghaei-Ghareh-Bolagh B, Dang TT, Topkaya SN, Gao X, Yang SY, Jung SM, Oh JH, Dokmeci MR, Tang XS, Khademhosseini A. Cell-laden microengineered and mechanically tunable hybrid hydrogels of gelatin and graphene oxide. Adv Mater. 2013; 25:6385–6391. [PubMed: 23996513]
43. Singh S, Singh AN, Verma A, Dubey VK. Biodegradable polycaprolactone (PCL) nanosphere encapsulating superoxide dismutase and catalase enzymes. Appl Biochem Biotechnol. 2013; 171:1545–1558. [PubMed: 23975280]
44. Sokolovic D, Djordjevic B, Kocic G, Veljkovic A, Marinkovic M, Basic J, Jevtovic-Stoimenov T, Stanojkovic Z, Sokolovic DM, Pavlovic V, Djindjic B, Krstic D. Melatonin protects rat thymus against oxidative stress caused by exposure to microwaves and modulates proliferation/apoptosis of thymocytes. Gen Physiol Biophys. 2013; 32:79–90. [PubMed: 23531837]
45. Stephens EH, Durst CA, West JL, Grande-Allen KJ. Mitral valvular interstitial cell responses to substrate stiffness depend on age and anatomic region. Acta Biomater. 2011; 7:75–82. [PubMed: 20624493]
46. Syedain Z, Reimer J, Schmidt J, Lahti M, Berry J, Bianco R, Tranquillo RT. 6-Month aortic valve implantation of an off-the-shelf tissue-engineered valve in sheep. Biomaterials. 2015; 73:175–184. [PubMed: 26409002]
47. Tseng H, Cuchiara ML, Durst CA, Cuchiara MP, Lin CJ, West JL, Grande-Allen KJ. Fabrication and mechanical evaluation of anatomically-inspired quasilaminate hydrogel structures with layer-specific formulations. Ann Biomed Eng. 2013; 41:398–407. [PubMed: 23053300]
48. Tseng H, Puperi DS, Kim EJ, Ayoub S, Shah JV, Cuchiara ML, West JL, Grande-Allen KJ. Anisotropic Poly(Ethylene Glycol)/Polycaprolactone Hydrogel-Fiber Composites for Heart Valve Tissue Engineering. Tissue Eng Part A. 2014
49. Wang H, Sridhar B, Leinwand LA, Anseth KS. Characterization of cell subpopulations expressing progenitor cell markers in porcine cardiac valves. PLoS One. 2013; 8:e69667. [PubMed: 23936071]
50. Williams CG, Malik AN, Kim TK, Manson PN, Elisseeff JH. Variable cytocompatibility of six cell lines with photoinitiators used for polymerizing hydrogels and cell encapsulation. Biomaterials. 2005; 26:1211–1218. [PubMed: 15475050]
51. Zhu J. Bioactive modification of poly(ethylene glycol) hydrogels for tissue engineering. Biomaterials. 2010; 31:4639–4656. [PubMed: 20303169]

Author Manuscript Author Manuscript Author Manuscript Author Manuscript

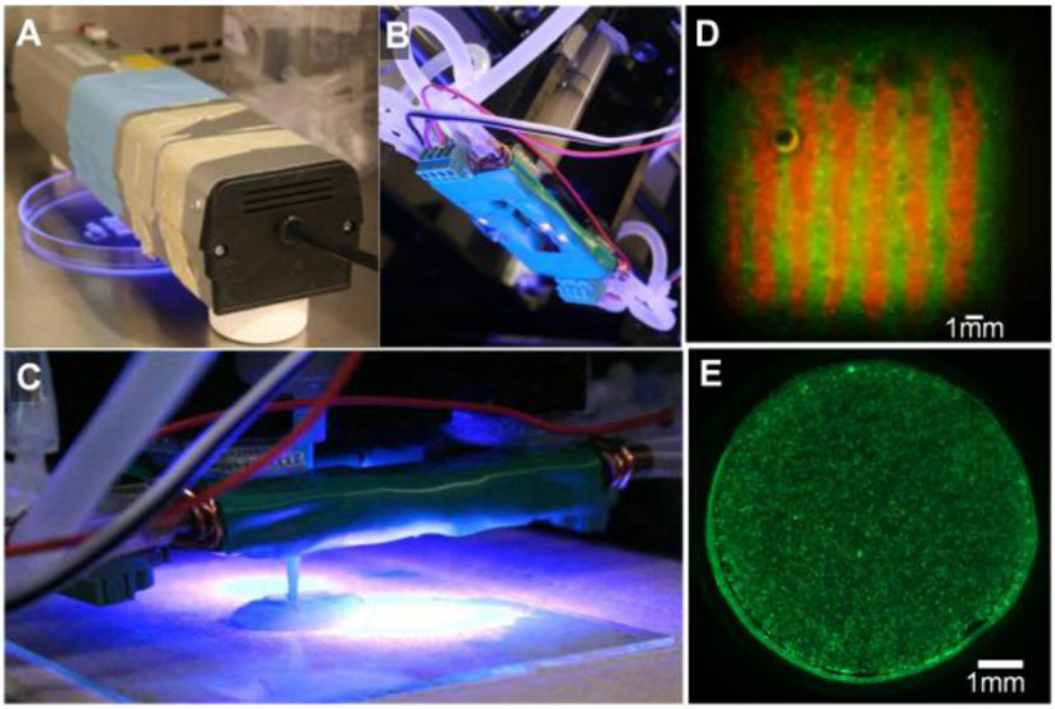

FIGURE 1.

High and low intensity 365 nm light sources were used to photocrosslink hydrogel precursor solution encapsulating living cells. (A) For the low intensity light condition a Spectroline Lamp 365 nm EN280L single bulb, 2.0 mW/cm^2 was used, and (B) for the high intensity condition a High Powered 4 LED Array with circulation heat sink, 136 mW/cm^2 was used (under-side view). (C) The high powered LED array mounts on the-Fab@Home Model 1 3D printing platform printer carriage, and is shown here with tip in contact with the printing surface (side-view). At this distance the light intensity at the printing surface is 136 mW/cm^2. (D) MEGEL/PEGDA3350/Alginate hydrogel precursor solution was combined with cells as an extrudable ink. Shown here is a cell-laden square prism with internal lined heterogeneity that was bioprinted and photocrosslinked. In this example print HADMSC were labeled with either CellTracker™ Red CMTPX or Green CMFDA and the bioprinted prism was photocrosslinked for 5 minutes at 2 mW/cm^2 and then cultured for 3 days. (E) To test assess the effects of variables associated with photocrosslinking cell ink precursor solutions were photocrosslinked into a simple disk geometry. Shown here is a representative image of a hydrogel disk containing HADMSC stained with calcein AM at day 3 of culture (precursor solution prepared with 0.05 w/v% Irgacure and exposed to lamp (2 mw/cm^2) for 5 minutes).

Author Manuscript Author Manuscript Author Manuscript Author Manuscript

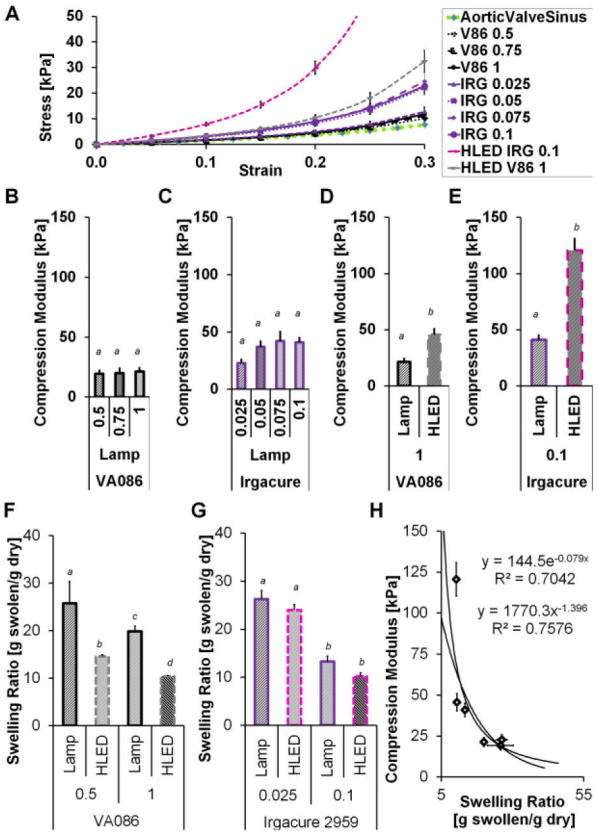

FIGURE 2.

Compression modulus (E_{5to15}) and swelling ratio of photocrosslinked hydrogels. Error bars are standard error of the mean, and $p<0.05$ non-matching letters. (A)Stress verses strain for hydrogels loaded with uniaxial compression. (B–E) Compressive modulus of crosslinked hydrogels made with variable photoinitiator type, concentration and light source during crosslinking. These conditions were photocrosslinked under either a lamp or high powered LED array (HLED) for 5 minutes (2 or 136 mW/cm^2). (B) E_{5to15} of hydrogels formed from precursor solutions prepared with three different concentrations of VA086 photoinitiator and crosslinked under a lamp for 5 minutes. One-way ANOVA with post-hoc Tukey-Kramer HSD (honest significant difference) test showed no significant between photoinitiator concentrations. (C) E_{5to15} of hydrogels formed from precursor solutions prepared with four different concentrations of Irgacure photoinitiator and crosslinked under a lamp for 5 minutes. One-way ANOVA with post-hoc Tukey-Kramer HSD test showed no significant between photoinitiator concentrations. (D) E_{5to15} of hydrogels formed from precursor solutions prepared with 0.1%w/v of Irgacure and crosslinked under a lamp or HLED for 5 minutes. One-way ANOVA with post-hoc Tukey-Kramer HSD test, $p=0.0021$ between lamp and HLED crosslinked conditions. (E) E_{5to15} of hydrogels formed from precursor solutions prepared with 1.0%w/v of VA086 and crosslinked under a lamp or HLED for 5 minutes. One-way ANOVA with post-hoc Tukey-Kramer HSD test, $p<0.0001$ between lamp and HLED crosslinked conditions. (B–E) Compressive modulus averages for the data shown are listed in Table S2. (F) Weight based swelling ratio (swollen weight divided by dry weight) of crosslinked hydrogels made with variable VA086 concentration and crosslinking light

Author Manuscript Author Manuscript Author Manuscript Author Manuscript

source. A two-way ANOVA showed no statistically significant interaction between the effect of VA086 concentration and the effect of light source on hydrogel swelling ratio ($F=0.4151$ $p=0.4151$), but both photoinitiator concentration and light source independently affect the swelling ratio. Results of Tukey HSD post-hoc test $p<0.05$ shown with non-matching letters. Average swelling ratios are listed in Table S3 and two-way ANOVA results are in Table S6. (G) Weight based swelling ratio of crosslinked hydrogels made with variable Irgacure concentration and light source during crosslinking. A two-way ANOVA showed no statistically significant interaction between the effect of Irgacure concentration and the effect of light source on hydrogel swelling ratio ($F=0.1101$ $p=0.7428$), but both photoinitiator concentration and light source independently affect the swelling ratio (two-way ANOVA results are in Table S7). Results of Tukey HSD post-hoc test $p<0.05$ shown with non-matching letters. (H) Compressive modulus versus swelling ratio of hydrogels.

Author Manuscript Author Manuscript Author Manuscript Author Manuscript

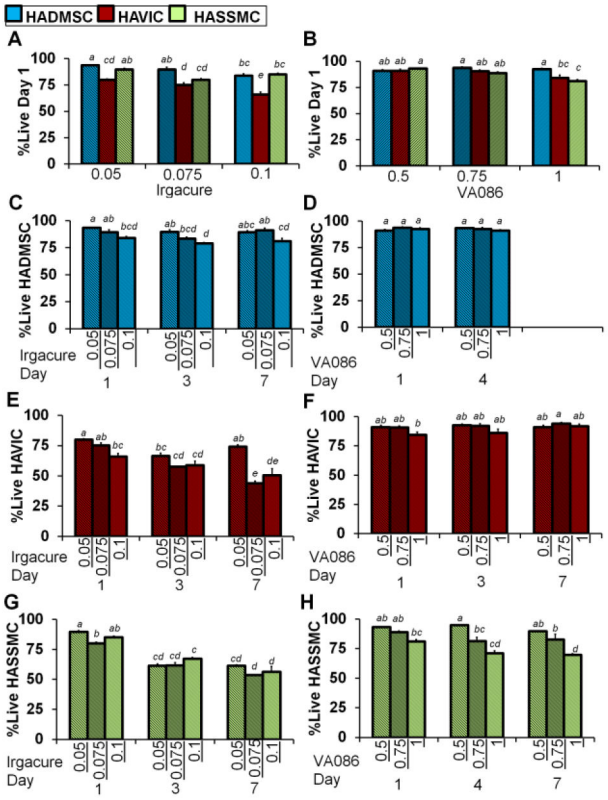

FIGURE 3.

Percentage of live cells in photocrosslinked hydrogels at low (2 mw/cm^2) light intensity. (A and B) Percentage of live encapsulated HADMSC, HAVIC, HASSMC stained with Live/Dead at day 1 of culture. Precursor solution was made with increasing (A) Irgacure 2959 and (B) VA086 concentrations and crosslinked with a lamp at 2 mW/cm^2 and compared between cell types. Average live percentage values for day 1 are listed in Table S2, and representative Live/Dead images of each condition are in supplemental materials (Fig. S2–S7). Results of two-way ANOVA listed in Table S8 and Table S9. Non-matching letters on graph indicate $p<0.05$ for Tukey HSD post-hoc test and standard error of the mean shown by error bars. (A) At day 1 in culture there was a statistically significant interaction between the effect of cell type and the effect of photoinitiator concentration on the percentage of live cells in the Irgacure hydrogels ($F=5.894$ $p=0.0015$). (B) At day 1 in culture there was a statistically significant interaction between the effects of cell type and VA086 photoinitiator concentration on the percentage of live cells ($F=3.96$ $p=0.0127$). (C–H) Encapsulated HADMSC, HAVIC, HASSMC were also stained with Live/Dead at day 3, 4, or 7 of culture. Two-way ANOVA were conducted to examine the effect of photoinitiator concentration and day in culture on the percentage of live cells for (C) HADMSC in Irgacure hydrogels, Table S10, (C) HADMSC in VA086 hydrogels, Table S11, (E) HAVIC in Irgacure hydrogels, Table S12 (F) HAVIC in VA086 hydrogels, Table S13, (G) HASSMC in Irgacure hydrogels, Table S14, (H) HASSMC in VA086 hydrogels, Table S15. Non-matching letters on graphs indicate $p<0.05$ for Tukey HSD post-hoc test and standard error of the mean shown by error bars. For HADMSC there was not a statistically significant interaction between the effects of

Author Manuscript Author Manuscript Author Manuscript Author Manuscript

photoinitiator concentration and day in culture on the percentage of live cells in hydrogels prepared with Irgacure ($F=1.555$ $p=0.2149$) or VA086 concentration and day in culture on the percentage of live cells ($F=1.771$ $p=0.0.2002$). There was a statistically significant interaction between the effects of day in culture and photoinitiator concentration on the percentage of live HAVIC for Irgacure ($F=7.165$ $p=0.0005$) but not VA086 ($F=1.284$ $p=0.3018$) hydrogels. There was a statistically significant interaction between the effects of day in culture and photoinitiator concentration on the percentage of live HASSMC for Irgacure hydrogels ($F=3.9815$ $p=0.0124$) but not VA086 ($F=1.6005$ $p=0.204$) hydrogels.

Author Manuscript Author Manuscript Author Manuscript Author Manuscript

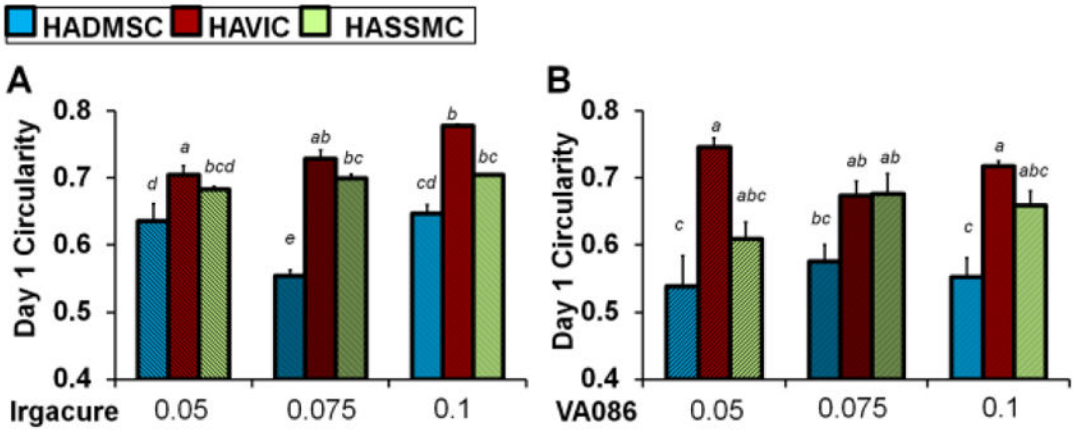

FIGURE 4.

Circularity of encapsulated HADMSC, HAVIC, and HASSMC stained with calcein-AM at day 1 of culture. Hydrogel precursor solution was made with increasing (A) Irgacure 2959 and (B) VA086 concentration and photocrosslinked with a Lamp at 2 mW/cm^2. Average circularity values for day 1 are listed in Table S2. Results of two-way ANOVA are summarized in Table S16 and Table S17. Non-matching letters on the graphs indicate $p<0.05$ for Tukey HSD post-hoc test and standard error of the mean shown by error bars. At day 1 in culture there was a statistically significant interaction between the effect of cell type and the effect of Irgacure photoinitiator concentration on the circularity of live cells ($F=7.5042$ $p=0.0003$, Table S16). At day 1 in culture there was not a statistically significant interaction between the effect of cell type and the effect of VA086 photoinitiator concentration on the circularity of live cells ($F=1.8884$ $p=0.1438$, Table S17) but the circularity of cells in VA086 hydrogels does depend on the cell type ($p<0.0001$).

Author Manuscript Author Manuscript Author Manuscript Author Manuscript

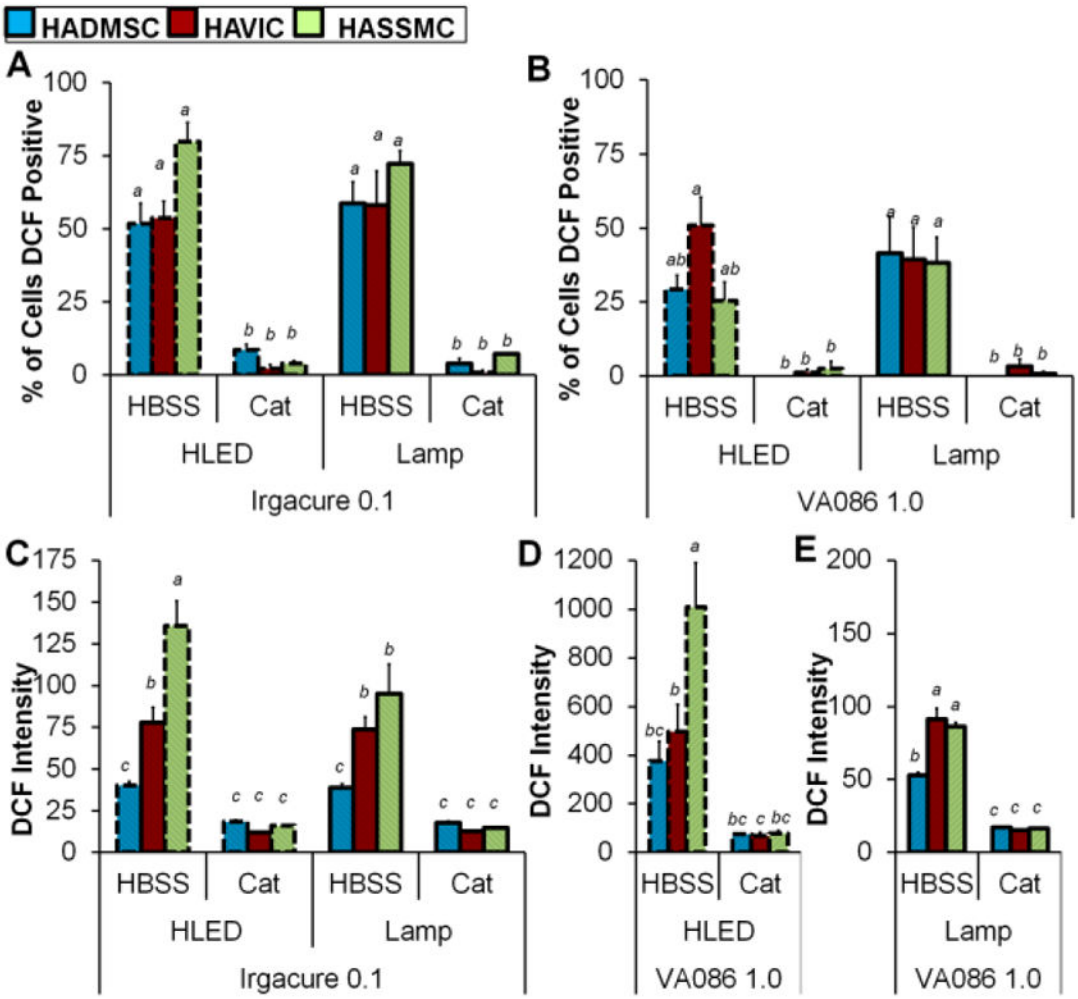

FIGURE 5.

Oxidative stress differences between HAVIC, HASSMC, and HADMSC that were treated with HBSS (control) or catalase then photo-encapsulated. (A) Percent of encapsulated cells in Irgacure hydrogels that are DCF positive and experiencing general oxidative stress after photo-crosslinking with lamp 2 mW/cm^2 and high powered LED 136 mW/cm^2. Results of three-way ANOVA indicate there was not a statistically significant interaction between the effect of light intensity, the effect of cell type, and the effect of treatment on the percentage of DCF positive cells (F=0.46 p=0.46, Table S18). (B) Percent of encapsulated cells in VA086 hydrogels that are DCF positive and experiencing general oxidative stress after photo-crosslinking with lamp 2 mW/cm^2 and high powered LED 136 mW/cm^2. There was not a statistically significant interaction between the effect of light intensity, the effect of cell type, and the effect of treatment on the percentage of DCF positive cells (three-way ANOVA F=1.44 p=0.25, Table S19). (C) Relative fluorescent signal of DCF general oxidative stress indicator in Irgacure hydrogel encapsulated HAVIC, HASSMC, and HADMSC samples crosslinked with high powered LED array 136 mW/cm^2 and lamp 2 mW/cm^2. Three-way ANOVA indicates there was not a statistically significant interaction between the effect of light intensity, the effect of cell type, and the effect of treatment on the percentage of DCF

Author Manuscript Author Manuscript Author Manuscript Author Manuscript

positive cells (F=2.30 p=0.0647, Table S20). Relative fluorescent signal of DCF general oxidative stress indicator in VA086 hydrogel encapsulated HAVIC, HASSMC, and HADMSC samples crosslinked with (D) high powered LED array 136 mW/cm^2 and (E) lamp 2 mW/cm^2. The VA086 photoinitiator foams the hydrogel upon photocrosslinking, and the HLED/VA086 condition is significantly more buoyant compared to the lamp/VA086 conditions soon after photocrosslinking. As a result the HLED/VA086 condition fluorescence signal is more intense due to the higher buoyancy of the hydrogels. (D) Two-way ANOVA indicates there was a statistically significant interaction between the effect of cell type and the effect of treatment on the percentage of DCF positive cells in hydrogels prepared with Irgacure (F=6.30 p=0.0085, Table S21). (E) There was a statistically significant interaction between the effect of cell type and the effect of treatment on the percentage of DCF positive cells in hydrogels prepared with VA086 (F=22.7 p<0.0001, Table S22). For all graphs (A–D) non-matching letters on the graphs indicate p<0.05 for Tukey HSD post-hoc test and error bars indicate standard error of the mean. Representative confocal images of DCF and CTR stained cells are in supplemental materials (Fig. S8), and fluorescence averages are listed in Table S4.

Author Manuscript Author Manuscript Author Manuscript Author Manuscript

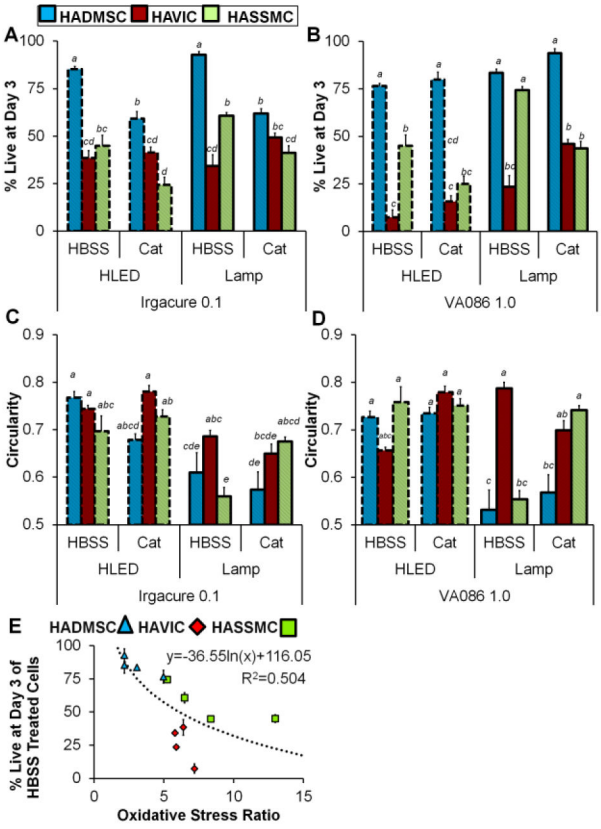

FIGURE 6.

Effect of catalase loading on HAVIC, HASSMC, and HADMSC cell viability and circularity. Cells were treated with catalase or HBSS (control) before encapsulation and light exposure. (A) Percentage of live cells encapsulated in Irgacure 0.1%w/v hydrogel disks and cultured for 3 days after photo-crosslinking with lamp 2 mW/cm^2 and high powered LED 136 mW/cm^2. Results of three-way ANOVA indicate there was not a statistically significant interaction between the effect of light intensity, the effect of cell type, and the effect of treatment on the percentage of live cells (F=1.41 p=0.26, Table S23), but there was a significant interaction between effect of cell type and effect of catalase treatment (F=29.44 p=<0.0001). (B) Percentage of live cells encapsulated in VA086 1.0%w/v hydrogel disks and cultured for 3 days after photo-crosslinking with lamp and high powered LED. There was not a statistically significant interaction between the effect of light intensity, the effect of cell type, and the effect of treatment on the percentage of live cells (F=1.5470 p=0.2271, Table S24), but there was a significant interaction between effect of cell type and effect of catalase treatment (F=17.4736 p=<0.0001). (C) Circularity of live of cells encapsulated in Irgacure 0.1%w/v hydrogel disks and cultured for 3 days after photo-crosslinking with lamp and high powered LED array. There was a statistically significant interaction between the effect of catalase treatment, the effect of light intensity, and the effect of cell type (F=3.469 p=0.0419, Table S25). (D) Circularity of live cells encapsulated in VA086 1.0%w/v hydrogel disks and cultured for 3 days after photo-crosslinking with lamp and high powered LED array. There was a statistically significant interaction between the effect of catalase treatment, the effect of light intensity, and the effect of cell type (F=13.5989 p<0.0001, Table S26). For all graphs

Author Manuscript Author Manuscript Author Manuscript Author Manuscript

(A–D) non-matching letters on the graphs indicate $p<0.05$ for Tukey HSD post-hoc test and error bars indicate standard error of the mean. Viability and circularity averages are listed in Table S5, and representative live/dead images are in the supplement (Fig. S10). (E) Viability versus oxidative stress ratio for HBSS (control) treated HAVIC, HASSMC, and HADMSC in photo-encapsulation conditions including both lamp and high powered LED array crosslinking.

Author Manuscript Author Manuscript Author Manuscript Author Manuscript

TABLE 1

Damage to mechanics ratio

The decrease in cell viability corresponding to a jump in photoinitiator radicals induced by increasing the light intensity was divided by the increase in mechanical properties to give a damage to mechanical gain ratio.

Light Intensity [mW/cm^2]	Photo-initiator [w/v%]	Modulus [kPa]	Cell Type	Oxidative Stress Ratio	Viability [%]	Damage/ Mechanic Ratio [%]/[kPa]
2 to 136	***VA086 1.0***	19.3±2.8 to 45.6±5.2	*HAVIC*	5.90 to 7.21	23.4±3.4 to 7.43±1.2 NSD	16/26= 0.62*
			HASSMC	5.25 to 12.97	74.4±2.9 to 45.1±4.6	29/26= 1.1*
			HADMSC	3.06 to 4.98	83.5±4.8 to 76.5±6.1 NSD	7/26= 0.27
	Irgacure 2959 0.1	40.9±4.1 to 120.7±10.2	*HAVIC*	5.79 to 6.40	49.2±2.4 to 41.3±3.0 NSD	8/80= 0.10
			HASSMC	6.49 to 8.37	62.0±1.8 to 44.8±5.7 NSD	18/80= 0.23
			HADMSC	2.17 to 2.17	92.7±1.7 to 85.2±1.4 NSD	8/80= 0.10